

# Two-moment Bulk Stratiform Cloud Microphysics in the Grid-point Atmospheric Model of IAP LASG (GAMIL)

SHI Xiangjun<sup>\*1,2,3</sup> (史湘军), WANG Bin<sup>1</sup> (王斌), Xiaohong LIU<sup>4</sup>, and Minghuai WANG<sup>4</sup>

<sup>1</sup>*State Key Laboratory of Numerical Modeling for Atmospheric Sciences and Geophysical Fluid Dynamics,  
Institute of Atmospheric Physics, Chinese Academy of Sciences, Beijing 100029*

<sup>2</sup>*Hebei Key Laboratory for Meteorology and Eco-environment, Shijiazhuang 050021*

<sup>3</sup>*Hebei Climate Center, Shijiazhuang 050021*

<sup>4</sup>*Pacific Northwest National Laboratory, Richland, Washington, USA*

(Received 17 April 2012; revised 20 September 2012)

## ABSTRACT

A two-moment bulk stratiform microphysics scheme, including recently developed physically-based droplet activation/ice nucleation parameterizations has been implemented into the Grid-point Atmospheric Model of IAP LASG (GAMIL) as an effort to enhance the model's capability to simulate aerosol indirect effects. Unlike the previous one-moment cloud microphysics scheme, the new scheme produces a reasonable representation of cloud particle size and number concentration. This scheme captures the observed spatial variations in cloud droplet number concentrations. Simulated ice crystal number concentrations in cirrus clouds qualitatively agree with in situ observations. The longwave and shortwave cloud forcings are in better agreement with observations. Sensitivity tests show that the column cloud droplet number concentrations calculated from two different droplet activation parameterizations are similar. However, ice crystal number concentration in mixed-phased clouds is sensitive to different heterogeneous ice nucleation formulations. The simulation with high ice crystal number concentration in mixed-phase clouds has less liquid water path and weaker cloud forcing. Furthermore, ice crystal number concentration in cirrus clouds is sensitive to different ice nucleation parameterizations. Sensitivity tests also suggest that the impact of pre-existing ice crystals on homogeneous freezing in old clouds should be taken into account.

**Key words:** two-moment cloud microphysics scheme, atmospheric model

**Citation:** Shi, X. J., B. Wang, X. H. Liu, and M. H. Wang, 2013: Two-moment bulk stratiform cloud microphysics in the Grid-point Atmospheric Model of IAP LASG (GAMIL). *Adv. Atmos. Sci.*, **30**(3), 868–883, doi: 10.1007/s00376-012-2072-1.

## 1. Introduction

Although the importance of clouds in climate system is well known (Arakawa, 2004), cloud representation in general circulation models (GCMs) remains a challenge due to the vast range of temporal and spatial scales in cloud processes (Iacono et al., 2008; Morrison and Gettelman, 2008). Thus, clouds are considered a major source of uncertainty in climate simulations (IPCC, 2007).

With increasing computing power, cloud parameterizations are becoming more sophisticated, and cloud

processes have been treated in more realistic manners. Whereas substantial simplifications still need to be made in simulating cloud formation and evolution in higher-resolution cloud-resolving models, the large grid spacing of GCMs introduces additional challenges, such as treatment of cloud condensation and cloud fraction. According to the size of GCM grid scales, cloud processes are generally divided into two categories: convective cloud and stratiform cloud processes. Convective cloud processes are treated with a highly simplified microphysics parameterization because their spatial scales are significantly smaller than

---

\*Corresponding author: SHI Xiangjun, xiangjun.10@gmail.com

the size of a grid cell in GCMs. On the other hand, large-scale, stratiform cloud processes can be treated with fairly detailed cloud microphysics parameterizations. A recent improvement in the representation of cloud processes in large-scale models has been the implementation of two-moment bulk stratiform microphysics schemes that predict two moments of cloud water/precipitation species and represent the particle size with a distribution function (Morrison and Pinto, 2005). Prediction of both cloud particle number concentration and mass mixing ratio enables the cloud particle size to evolve in a more consistent manner and thus improves the calculation of microphysical processes and radiative transfer (Meyers et al., 1997).

Furthermore, the development of two-moment cloud microphysics schemes allows us to analyze the complicated interactions between aerosols and clouds, and to further quantify the influence of aerosols on the microphysical and radiative properties of clouds, so-called aerosol indirect effects (Lohmann and Feichter, 2005; Ghan and Schwartz, 2007). Although climate models have been used to examine aerosol indirect effects for the last two decades, aerosol indirect effects remain one of the largest uncertainties in simulations of climate change (IPCC, 2007).

The root of aerosol indirect effects on warm clouds is the link between aerosol particles and droplets numbers. At the beginning of the last century, the theory of droplet nucleation (aerosol activation) was founded (Kohler, 1921). However, this theory cannot be applied in global models directly because the maximum supersaturation needed in the parameterization is not resolved in GCMs due to the coarse resolution. Historically, this issue has been addressed with empirical formulas that relate cloud droplet number concentrations with aerosol mass concentrations (Storelvmo et al., 2009). In recent years, physically-based droplet nucleation parameterizations that link cloud droplet number concentration to primary controlling parameters have been designed (e.g., Abdul-Razzak and Ghan, 2000; Nenes and Seinfeld, 2003). These physically-based parameterizations perform well under a wider variety of nucleation conditions (Ghan et al., 2011), and they have been widely used in global models, such as Community Atmospheric Model version 5 (CAM5) in the National Center for Atmospheric Research (NCAR), European Centre Hamburg model version 5 (ECHAM5) in Max-Planck-Institute (MPI), and Atmospheric Model version 3 (AM3) at Geophysical Fluid Dynamics Laboratory (GFDL) (Lohmann et al., 2007; Gettelman et al., 2008; Salzmann et al., 2010).

Compared to the aerosol effects on cloud droplet formation, the aerosol effects on ice crystal formation

are even more uncertain and less well understood (Liu et al., 2007; Barahona, 2008; Storelvmo et al., 2009; Jensen et al., 2010). Ice crystals can form by homogeneous freezing of aerosol solution particles or heterogeneous nucleation of ice on insoluble aerosol particles (Pruppacher and Klett, 1997). Homogeneous freezing occurs through ice germ formation within supercooled soluble aerosol particles at low temperature and high relative humidity. Heterogeneous ice nucleation include several modes (i.e., deposition, contact, immersion, and condensation) in which ice crystals form with the aid of so-called ice nuclei (IN). In general, the number concentration of soluble aerosol particles in the upper troposphere is significantly larger than IN. Homogeneous freezing usually generates a high number concentration of ice crystals, but heterogeneous nucleation does not. However, with the aid of IN, heterogeneous freezing tends to occur at lower supersaturation, depleting water vapor and hindering homogeneous freezing. In other words, heterogeneous nucleation would significantly reduce ice crystal number concentration compared to homogeneous freezing (Demott et al., 1994). Thus, the competition between homogeneous and heterogeneous nucleation could significantly change ice crystal number concentrations in cirrus clouds and yield potential IN effects on climate (Demott et al., 1997; Phillips et al., 2008; Barahona and Nenes, 2009a). The competition between homogeneous and heterogeneous nucleation also makes it challenging to design ice nucleation parameterizations. Recently, some physically-based parameterizations were presented (e.g., Liu and Penner, 2005; Barahona and Nenes, 2009a, b), and have been implemented into a few global models (e.g., Liu et al., 2007; Gettelman et al., 2010; Salzmann et al., 2010).

The goals of this study are to improve the representation of cloud microphysics processes in the Grid-point Atmospheric Model of IAP LASG (GAMIL) and to enhance the model's capability to simulate aerosol indirect effects. We incorporated a two-moment bulk cloud microphysics scheme into GAMIL. This new stratiform cloud scheme has been further improved by incorporating some recently developed physically-based droplet activation/ice nucleation parameterizations. Thus, we can investigate sensitivity of simulated radiative fluxes and cloud fields to different physically-based droplet activation/ice nucleation parameterizations. This paper is organized as follows: section 2 describes the new stratiform microphysics scheme; results from the new developed model are presented and evaluated in section 3; our investigation of the sensitivity of this two-moment stratiform cloud scheme to different droplet activation/ice nucleation parameterizations is presented in section 4; and conclusions are

given in section 5.

## 2. Model description

### 2.1 *An overview of the standard version of GAMIL*

The dynamical core of GAMIL is a grid-point framework developed by Wang et al. (2004). This dynamical core can maintain mass conservation and effective energy conservation. The resolution of this dynamical core is adjustable. A mass and shape-preserving advection scheme developed by Lin and Rood (1996) has been implemented into GAMIL by Zhang (2008). The physical package of GAMIL is similar to the Community Atmospheric Model version 3(CAM3) of NCAR (Collins et al., 2006). There are three convective cloud schemes in GAMIL: Zhang and McFarlane (1995), Zhang and Mu (2005) and Tiedtke (1989). The standard GAMIL model has been evaluated (Li et al., 2007; Yang et al., 2007) and applied (Li et al., 2008; Wu and Li, 2008) in climate change studies. Note that the GAMIL model focuses on East Asian climate. To improve its performance of East Asian climate simulation, GAMIL has been improved by upgrading the deep convection parameterization and the cumulus cloud fraction and by tuning some of the large uncertainty parameters. Compared with the CAM model, GAMIL demonstrates some improvements: the geographic distribution of the precipitation over East Asia, the response of atmosphere circulation to the tropical ocean, the eastward propagation, and spatial/temporal structures of the Madden Julian Oscillation (Li et al., 2013).

Here, we give a brief description of the one-moment stratiform cloud scheme in the standard GAMIL. Cloud fraction,  $C$ , is diagnosed as a function of relative humidity, following Slingo (1987):

$$C = \left( \frac{\text{RH} - \text{RH}_{\min}}{1 - \text{RH}_{\min}} \right)^2, \quad (1)$$

where RH is relative humidity, and threshold relative humidity  $\text{RH}_{\min}$  is an adjustable parameter. The condensation/evaporation of cloud water/ice is described in Rasch and Kristjánsson (1998). In this scheme (hereafter RK scheme), changes in water vapor and heat in a grid box are treated consistently with changes in cloud fraction and in-cloud condensation. The total condensate is partitioned into liquid and ice phases according to a linear function of temperature. Five processes convert condensate to precipitate: conversion of liquid water to rain, collection of cloud water by rain, auto-conversion of ice to snow, collection of ice by snow, and collection of liquid by snow. Each is treated with an individual parameterization. In the

one-moment stratiform cloud scheme, the number concentration of cloud droplets is prescribed:  $400 \text{ cm}^{-3}$  over land,  $150 \text{ cm}^{-3}$  over ocean, and  $75 \text{ cm}^{-3}$  over sea ice. The fall speed for droplets is  $1.5 \text{ cm s}^{-1}$  over land and  $2.8 \text{ cm s}^{-1}$  over ocean and sea ice. Over ocean and sea ice, the effective radius of cloud droplets,  $r_{\text{el}}$ , is specified to be  $20 \text{ }\mu\text{m}$ . Over land,  $r_{\text{el}}$  is determined using

$$r_{\text{el}} = \begin{cases} 10 & T > -10 \\ 10 - 10 \left( \frac{T + 10}{20} \right) & -30 < T < -10 \\ r_{\text{ei}} & T < -30 \end{cases} \quad (2)$$

where  $T$  is temperature in the unit of degree centigrade,  $r_{\text{ei}}$  is cloud ice effective radius, which is a function of pressure, and  $r_{\text{ei}}$  ranges from  $10 \text{ }\mu\text{m}$  to  $30 \text{ }\mu\text{m}$ .

A detailed description of cloud scheme can be found in Collins et al. (2006). In the following section, we introduce the new improvement in the stratiform cloud scheme.

### 2.2 *Description of the new cloud microphysics scheme*

#### 2.2.1 *Two-moment bulk cloud microphysics scheme*

The Morrison and Gettelman (2008) two-moment bulk cloud microphysics scheme (hereafter MG scheme) has been implemented in GAMIL. Compared to the previous one-moment microphysics scheme (RK scheme), this two-moment scheme provides a more robust framework for studying aerosol-cloud interaction. The MG scheme is described in detail in Morrison and Gettelman (2008) and is only briefly described here.

The cloud droplet and ice crystal size distributions are represented by gamma functions:

$$\phi(D) = N_0 D^\mu e^{-\lambda D}, \quad (3)$$

where  $D$  is diameter,  $N_0$  is the “intercept” parameter,  $\lambda$  is the slope parameter, and  $\mu$  is the spectra shape parameter.

The spectral parameters  $N_0$  and  $\lambda$  are derived from local in-cloud droplet number  $N''$  and mass mixing ratio  $q''$ :

$$\lambda = \left[ \frac{\pi \rho N'' \Gamma(\mu + 4)}{6 q'' \Gamma(\mu + 4)} \right]^{(1/3)}, \quad (4)$$

$$N_0 = \frac{N'' \lambda}{\Gamma(\mu + 1)}, \quad (5)$$

where  $\Gamma$  is the Euler gamma function and  $\rho$  is the density of cloud droplet and ice crystals:  $1000 \text{ kg m}^{-3}$  and  $500 \text{ kg m}^{-3}$  for cloud droplet and cloud ice, respectively.

Cloud droplet and ice crystal effective radius  $r_e$  used in the radiation parameterization scheme are obtained directly from the size distribution function of

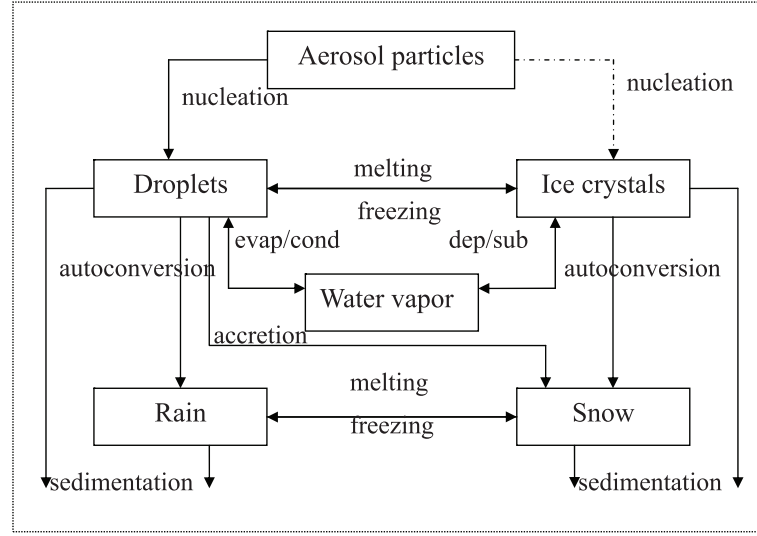


**Fig. 1.** Block schematic diagram for all cloud processes in the MG scheme.

Eq. (3):

$$r_e = \frac{\Gamma(\mu + 4)}{2\lambda(\mu + 3)}, \quad (6)$$

The mass- and number-weighted terminal fall speed for cloud droplets and ice crystals can also be obtained from size distribution function:

$$V_N = \frac{\left(\frac{\rho_a}{\rho_{a0}}\right)^{0.54} a\Gamma(\mu + 1 + b)}{\lambda^b \Gamma(\mu + 1 + b)}, \quad (7)$$

$$V_q = \frac{\left(\frac{\rho_a}{\rho_{a0}}\right)^{0.54} a\Gamma(\mu + 4 + b)}{\lambda^b \Gamma(\mu + 4 + b)}, \quad (8)$$

where  $V_q$  and  $V_N$  are mass- and number-weighted fall speed,  $\rho_a$  is air density,  $\rho_{a0}$  is the reference air density at the standard temperature and pressure, and  $a$  and  $b$  are empirical coefficients in the diameter–fall speed relationship.

The time evolution of mass mixing ratio and number concentration is determined by grid scale advection, convective detrainment, turbulent diffusion, and several microphysical processes (Fig. 1). A detailed description of this scheme can be found in Morrison and Gettelman (2008).

### 2.2.2 Several modifications

Besides the implementation of the MG scheme in GAMIL, several modifications have been made on the model physics of GAMIL. First, the mass mixing ratio and number concentration of cloud particles are added to the constituent transport by deep convection. Second, to reduce the high biases of total cloud cover over the polar region in a low water vapor mixing ratio environment, an empirical fit to observations of Arctic

clouds, which is described in more detail by (Vavrus and Waliser, 2008), is adopted to the Slingo scheme. Finally, the detrained cloud water from convection is no longer assumed to evaporate but is added to stratiform cloud water and ice. The fraction of ice water in the detrained condensate is a linear function of temperature between  $-40^\circ\text{C}$  and  $-10^\circ\text{C}$ . Number concentrations are calculated by assuming a mean volume radius of 16 and 32  $\mu\text{m}$  for detrained cloud droplets and cloud ice, respectively.

### 2.2.3 Droplet nucleation

In the MG scheme, activation of cloud droplets is treated with the physically-based parameterization developed by Abdul-Razzak and Ghan (2000, hereafter AG). The number of activated cloud droplets is considered a function of aerosol chemical and physical properties, ambient temperature, and vertical velocity. Activation of cloud droplets occurs if the in-cloud droplet number decreases below the diagnosed active cloud condensation nucleus (CCN) number. A sub-grid vertical velocity,  $W'$ , for calculating droplet nucleation can be derived from the turbulent diffusion coefficient following Morrison and Pinto (2005):

$$W' = \frac{k_d}{l_c}, \quad (9)$$

where  $k_d$  is the turbulent diffusion coefficient and  $l_c = 30$  m is the mixing length. A minimum sub-grid vertical velocity of  $0.1 \text{ m s}^{-1}$  is assumed for weak turbulent diffusion.

To examine the sensitivity of aerosol indirect effects to droplet nucleation parameterizations, we implemented another droplet activation parameterization by Nenes and Seinfeld (2003, hereafter NS) in

GAMIL. Compared to the AG parameterization, the concept of “population splitting” is introduced to this parameterization. CCN are divided into two separate populations: those that have a size close to their critical diameter and those that do not. The water vapor consumption by the growth of the former population can be neglected. The NS parameterization also explicitly introduces mass transfer (kinetic) limitations on droplet growth. Unlike the AG parameterization, the maximum supersaturation, below which aerosol particles with critical supersaturation would be activated, is solved by iteration rather than approximate functions. Therefore, it is more computationally costly than the AG parameterization, which slows down the GAMIL model by 5% compared to the AG parameterization.

#### 2.2.4 Ice nucleation

In the MG scheme, ice crystals nucleated in both ice clouds and mixed-phase clouds are calculated by the heterogeneous ice nucleation mechanism. IN is diagnosed from an empirical function of temperature following Cooper (1986). An upper limit of IN number is applied at  $-35^{\circ}\text{C}$  ( $0.209\text{ cm}^{-3}$ ). Homogeneous freezing of supercooled aerosol solution is not explicitly considered.

Two physically-based ice nucleation parameterizations, Liu and Penner (2005, hereafter LP) and Barahona and Nenes (2009a and b, hereafter BN), have been incorporated into the cloud scheme. These two parameterizations include homogeneous nucleation on sulfate and heterogeneous nucleation on mineral dust. The LP parameterization is derived by fitting the results from cloud parcel model experiments. The nucleated ice crystal number is computed based on aerosol number concentrations, temperature, humidity, and updraft velocity. Grid mean humidity for this parameterization is multiplied by a factor 1.2 to take sub-grid variability into account. A threshold relative humidity for homogeneous ice formation is assumed in this parameterization, which is considered a function of temperature and updraft velocity. Unlike the LP parameterization, the BN parameterization provides an analytical solution of governing equations and explicitly accounts for the competition effects between homogeneous and heterogeneous nucleation. In the BN parameterization, the “nucleation spectrum”, which describes IN number concentration from an aerosol population as a function of temperature and supersaturation, is allowed to follow any form (i.e., derived from classical nucleation theory or from observations). Because the parameterization is derived in the Lagrangian framework of an ascending parcel, it is necessary to apply the threshold relative humidity

for homogeneous ice formation used in the LP parameterization, to account for the probability of finding a cloud-forming parcel within the grid cell. Some recent studies have shown that aerosols rich with organic matter may become glassy below the glassy-transition temperature ( $\sim 205\text{ K}$ ), preventing homogeneous nucleation (Jensen et al., 2010). In addition, homogeneous freezing driven by gravity wave motion would produce a high ice crystal number concentration ( $1\text{--}10\text{ cm}^{-3}$ ), and such high concentrations have not been observed (Krämer et al., 2009). Box model simulations and 1-D model simulations have suggested that only heterogeneous nucleation scenarios result in ice number concentration close to observations (Froyd et al., 2009; Gensch et al., 2008). Therefore, homogeneous freezing of liquid aerosols is prohibited at low temperature ( $<205\text{ K}$ ). The main purpose of this artificial setting is to examine whether only heterogeneous nucleation scenarios can result in ice number concentration close to observations in a global model.

In mixed-phase clouds with temperatures greater than  $-37^{\circ}\text{C}$ , ice crystal formation is represented by heterogeneous ice nucleation. In addition to the Cooper formulation, the four heterogeneous nucleation spectra used in the BN parameterization are added to mixed-phase clouds: Meyers, PDG, PDA, and CNT (Table 1). Meyers and PDG formulations are derived from in situ measurements (Meyers et al., 1992; Phillips et al., 2007). The PDA, presented by Phillips et al. (2008), is a more comprehensive formulation that takes the aerosol surface area contribution into account. The CNT formulation is derived from the classical nucleation theory.

### 3. Results and model evaluation

#### 3.1 Simulation setup

The results from the GAMIL with the new cloud microphysics have been extensively evaluated and compared with the standard version. We have performed two model simulations: one from the standard GAMIL with Rasch and Kristjánsson (1998) one-moment cloud scheme (hereafter GAMIL-RK simulation), and the other from the newly developed GAMIL with the Morrison and Gettelman (2008) two-moment cloud scheme (hereafter GAMIL-MG simulation). In the GAMIL-MG simulation, droplet activation is derived from the AG parameterization; ice nucleation in cirrus clouds uses the BN parameterization; and ice nucleation in mixed-phase clouds is represented by the Cooper formulation. IN spectrum in the BN parameterization is represented by the PDA formulation. All simulations in this study are run at  $\sim 2.8^{\circ}\times 2.8^{\circ}$

**Table 1.** Heterogeneous nucleation formulations.  $N_{\text{het}}$  is the ice crystals number concentration from heterogeneous freezing. The functions  $H_{\text{dust}}(Si, T)$  for PDA is defined in Phillips et al. (2008), and the functions  $k_{\text{hom}}(0.2-Si)$  for CNT is defined in Barahona and Nenes (2009a, b).  $Si$  is the water vapor supersaturation ratio with respect to ice, and  $N_{\text{dust}}$  is the dust number concentration.

parameterization	$N_{\text{het}}(\text{m}^{-3})$
Cooper (1986), Cooper	$5e^{0.304(273.15-T)}$
Meyers et al. (1997), Meyers	$10^3 e^{-0.639+12.96Si}$
Phillips et al. (2007), PDG	$60e^{-0.639+12.96Si}$
Phillips et al. (2008), PDA	$N_{\text{dust}} \left[ 1 - \exp \left( -\frac{2}{3} H_{\text{dust}}(Si, T) \frac{N_{\text{het,PDG}}}{3.3 \times 10^5} \right) \right]$
Classical Nucleation Theory, CNT	$0.05 \left[ \min \left( \frac{Si}{0.2} N_{\text{dust}} e^{-0.0011k_{\text{hom}}(0.2-Si)}, N_{\text{dust}} \right) \right]$

horizontal resolution with 26 vertical levels and a 20-minute time step, using climatological sea surface temperatures. The Zhang and Mu (2005) convective cloud scheme is used for all simulations. Each simulation is run for five years after a model spin up of four months.

A prescribed aerosol climatology is used in droplet activation and ice nucleation. The aerosol data is derived from a three-dimensional aerosol simulation (Collins et al., 2001) that include sulfate, hydrophobic black carbon, hydrophilic black carbon, hydrophobic organic carbon, hydrophilic organic carbon, dust (four

bins, from 0.01 to 10  $\mu\text{m}$ ), and sea salt. Aerosol number concentrations are diagnosed from mass mixing ratio using prescribed lognormal size distributions, following Gettelman et al. (2008). Notably, many global climate models have coupled cloud microphysics with aerosol models that can simulate the full spatial and temporal evolution of aerosol mass and size distributions. Fortunately, an aerosol model developed by Zhang (2008) has been implemented in the GAMIL. This limitation in the current GAMIL model is being solved.

### 3.2 Annual global mean values

**Table 2.** Global annual mean results and observations. Shown in the table are liquid water path over ocean (LWP,  $\text{g m}^{-2}$ ) compared to SSM/I data (Greenwald et al., 1993; Weng and Grody, 1994), ice water path from stratiform cloud (IWP,  $\text{g m}^{-2}$ ) compared to ISCCP data (Storelvmo et al., 2008), grid-mean column-integrated cloud droplet number concentration (CDNUMC,  $1 \times 10^6 \text{ cm}^{-2}$ ) compared to AVHRR data (Han et al., 1998), shortwave cloud forcing (SWCF,  $\text{W m}^{-2}$ ) and longwave cloud forcing (LWCF,  $\text{W m}^{-2}$ ) compared to various satellite products (Scott et al., 1999; Loeb et al., 2009), total cloud cover (CLDTOT, %) compared to surface observations (Hahn et al., 1994), ISCCP (Rossow and Schiffer, 1999) and MODIS data (King et al., 2003), stratiform precipitation rate (PRECL,  $\text{mm d}^{-1}$ ) and total precipitation rate (PRECT,  $\text{mm d}^{-1}$ ) compared to Global Precipitation Climatology Project (Adler et al., 2003).

Simulations	GAMIL-RK	GAMIL-MG	OBS
LWP	59.7	67.1	63–81
IWP	8.77	4.61	26.7
CDNUMC		2.74	4
SWCF	−34.2	−51.5	−46–−53
LWCF	21.7	22.5	22–31
CLDTOT	63.5	54.7	62–67
PRECL	0.74	0.57	
PRECT	3.05	3.03	2.61

Various global annual mean diagnostics are listed in Table 2. Liquid water path (LWP) and ice water path (IWP) are considered only for stratiform clouds, which includes the contribution from the convective detrainment. Satellite retrieved LWP on the global annual mean over the oceans ranges between 63  $\text{g m}^{-2}$  and 81  $\text{g m}^{-2}$ . The GAMIL-MG simulation with the two-moment scheme has a value (67.1  $\text{g m}^{-2}$ ) within this range, while the LWP is slightly underestimated in the GAMIL-RK simulation (59.7  $\text{g m}^{-2}$ ). The global mean IWP, derived from the International Satellite Cloud Climatology Project (ISCCP) including data from land and ocean, amounts to 26.7  $\text{g m}^{-2}$ . IWP in both GAMIL-RK (8.7  $\text{g m}^{-2}$ ) and GAMIL-MG (4.6  $\text{g m}^{-2}$ ) simulations are significantly less than the ISCCP retrievals, which is problematic for most GCMs (?). Notably, it is not clear how much ISCCP IWP includes precipitating ice particles (snow) as no global observation has yet been able to distinguish different ice hydrometeors, and the simulated IWP does not take snow and convective cloud condensate into account. In addition, IWP in the MG scheme strongly depends on the threshold crystal size used to distinguish ice crystal from snow particles, which is still very uncertain. Besides, a recent study by Liu et al. (2007) showed that IWP would be enhanced when a water va-

por deposition scheme was added to replace the fractional cloud closure scheme.

The global mean vertically integrated column-integrated cloud droplet number concentration (CDNUMC) as derived from the Advanced Very High Resolution Radiometer (AVHRR) data is  $4.0 \times 10^6 \text{ cm}^{-2}$  (Han et al., 1998). The CDNUMC in GAMIL-MG simulation is  $2.74 \times 10^6 \text{ cm}^{-2}$ . Notably, the simulated CDNUMC is sampled over clear and cloudy periods, and the satellite-retrieved CDNUMC is sampled only over cloudy periods and over the cloudy part (Lohmann, 2008). Thus, it is reasonable that the simulated CDNUMC ( $2.7 \times 10^6 \text{ cm}^{-2}$ ) is significantly smaller than the retrieved CDNUMC ( $4.0 \times 10^6 \text{ cm}^{-2}$ ).

The most striking difference between global annual mean results from RK and MG cloud microphysics scheme is a significant enhancement in short-wave cloud forcing (SWCF) in GAMIL-MG simulation. This increased SWCF ( $-51.5 \text{ W m}^{-2}$ ) lies within the uncertainty range ( $-46$ – $-53 \text{ W m}^{-2}$ ) from observations, while the SWCF from GAMIL-RK simulation ( $-34.2 \text{ W m}^{-2}$ ) is underestimated. Although IWP from GAMIL-MG simulation is smaller than GAMIL-RK simulation, LWP is larger in GAMIL-MG simulation than GAMIL-RK simulation. Even though IWP can be important to SWCF, SWCF is primarily determined by LWP, which may partly explain why the magnitude of SWCF is larger in the GAMIL-MG simulation. Another factor in determining SWCF is droplet effective radius. The cloud droplet effective radius calculated by the two-moment MG cloud scheme ( $<10 \text{ }\mu\text{m}$  at middle and low latitudes) is less than the specified values in the one-moment RK cloud scheme (range:  $10$ – $20 \text{ }\mu\text{m}$ ). This is the main reason that SWCF is significantly increased in GAMIL-MG simulation. There is a slight difference in longwave cloud forcing (LWCF). LWCF from GAMIL-MG simulation ( $22.5 \text{ W m}^{-2}$ ) was enhanced by  $0.73 \text{ W m}^{-2}$ , which results in slightly better agreement with the satellite observations ( $22$ – $31 \text{ W m}^{-2}$ ).

The total cloud cover decreases from 63.5% in GAMIL-RK to 54.7% in the GAMIL-MG run. The reduction in cloud fraction is mainly related to the modification of cloud fraction scheme. This modification is designed to reduce a bias of nearly 100% cloud cover in the polar region. As a result, the global mean cloud cover is decreased.

Although the total precipitation rate (PRECT) is similar in both simulations, the contribution from stratiform cloud (PRECL) decreases in GAMIL-MG simulation. One probable reason is that the smaller cloud droplets radius in GAMIL-MG simulation leads to less efficient precipitation production in stratiform clouds by slowing down the autoconversion of cloud

water to rain.

### 3.3 Annual zonal mean

Zonal mean LWCF and SWCF in both simulations qualitatively agree with observations from the Clouds and the Earth's Radiant Energy System (CERES) retrievals (Figs. 2a and b). LWCF is similar in both simulations, except for polar region due to the modification of cloud fraction scheme. The increased SWCF in GAMIL-MG simulation shows a much better agreement with observations at mid- and high-latitudes. The difference in SWCF between GAMIL-MG and GAMIL-RK simulations is related to the change in cloud droplet effective radius as discussed previously.

The zonal mean cloud cover from GAMIL-MG simulation agrees better with observation as the bias of near 100% cloud cover over polar region is reduced. However, cloud cover is underestimated in the high latitudes. One possible reason is that grid scale advection does not perform well over polar region as a result of larger meridional grid interval in the high latitudes than in the tropics. The precipitation is very similar in the two simulations with maxima in the tropics and in the mid-latitudes. It is interesting to note that the zonal distributions of precipitation rate in these two simulations are almost identical, while the stratiform precipitation rate in GAMIL-MG is substantially smaller than GAMIL-RK.

### 3.4 Annual latitude-pressure cross sections

The vertical structures of GAMIL-MG simulated particle size and in-cloud number concentration for cloud liquid and cloud ice are shown in Fig. 3. Low clouds have higher droplet number concentrations at  $\sim 900 \text{ hPa}$  than at higher altitudes (Fig. 3a). Furthermore, cloud droplet number concentrations are higher with high aerosol loading in the NH. In particular, cloud droplet number concentrations peak at  $40^\circ\text{N}$ , with a maximum of  $>140 \text{ cm}^{-3}$ . This value is close to observations over East Asia, as the droplet number concentrations derived from in situ measurements over East Asia is  $120.9 \text{ cm}^{-3}$  (Yin et al., 2011). Clouds with high aerosol loading result in a smaller cloud droplet effective radius. The smallest values are in the NH mid-latitudes, with values  $<8 \text{ }\mu\text{m}$ . For ice clouds, ice crystal number concentration peaks in the upper troposphere at  $\sim 200 \text{ hPa}$ . Cloud ice effective radius increases toward Earth's surface, with higher altitude cirrus clouds having smaller sizes ( $20 \text{ }\mu\text{m}$  radius) and mixed-phase clouds having larger sizes ( $60$ – $80 \text{ }\mu\text{m}$  radius) at lower altitudes.

The vertical structure of homogeneous nucleation occurrence frequency (i.e., count 1 if homogeneous

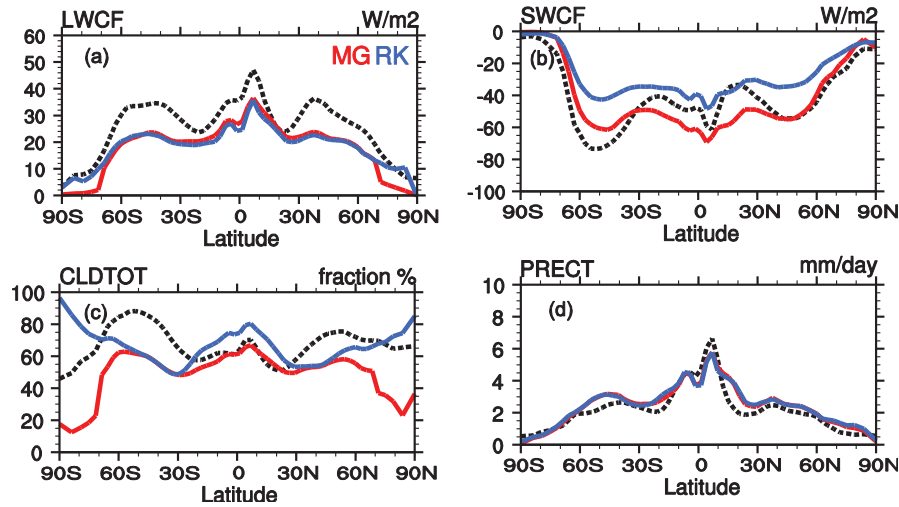


**Fig. 2.** Annual zonal mean of (a) longwave cloud forcing (LWCF,  $\text{W m}^{-2}$ ), (b) shortwave cloud forcing (SWCF,  $\text{W m}^{-2}$ ), (c) total cloud cover (CLDTOT, %) and (d) total precipitation (PRECT,  $\text{mm d}^{-1}$ ). Dotted black line refers to CERES data for cloud forcing, to ISCCP data for cloud cover and to XIE-ARKIN data (Xie and Arkin, 1997) for precipitation. Red line refers to GAMIL-MG simulation, and blue line refers to GAMIL-RK simulation.

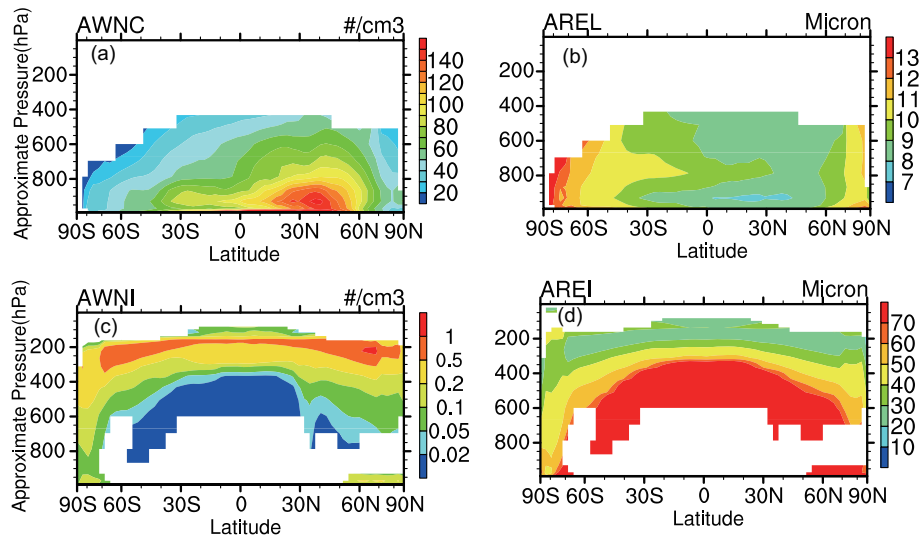


**Fig. 3.** Annual zonal mean of (a) in-cloud droplet number concentration (AWNC,  $\text{cm}^{-3}$ ), (b) cloud drop effective radius (AREL,  $\mu\text{m}$ ), (c) in-cloud ice crystal number concentration (AWNl,  $\text{cm}^{-3}$ ) and (d) cloud ice effective radius (AREI,  $\mu\text{m}$ ).

nucleation occurs, otherwise count 0 at each three-dimensional grid) is shown in Fig. 4a. The frequency distribution of ice nucleation occurrence events (i.e., in-cloud ice number concentration diagnosed from parameterization) is shown in Fig. 4b. Homogeneous freezing tends to occur at low temperature and high relative humidity, so that the occurrence frequency of homogeneous nucleation peaks in the upper troposphere

(Fig. 4a). The occurrence frequency of ice nucleation also peaks in the upper troposphere (Fig. 4b). We can see that most ice nucleation events in the upper troposphere at  $\sim 300$  hPa include homogeneous freezing, while few ice nucleation events in the middle troposphere above 400 hPa include homogeneous freezing. Figures 4c and d shows the diagnosed ice crystal number concentration from homogeneous nucleation and heterogeneous nucleation. The ice number concen-

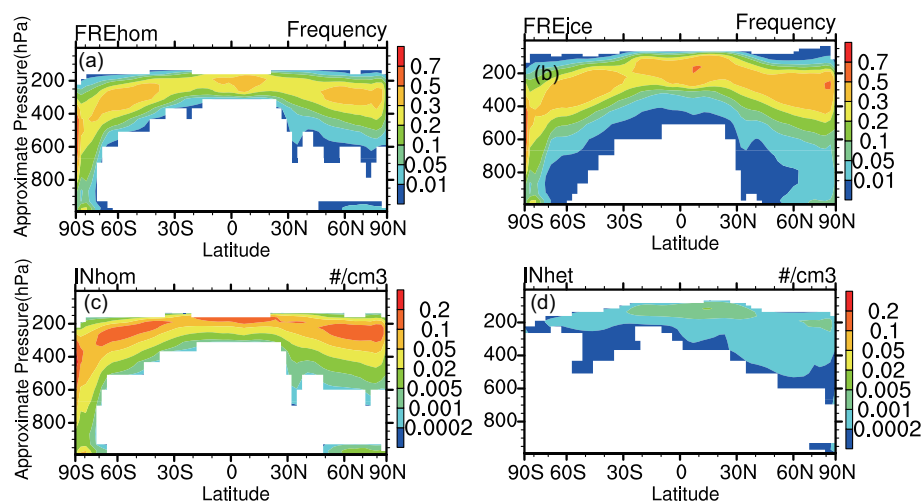


**Fig. 4.** Occurrence frequency of (a) homogeneous nucleation and (b) ice nucleation events. Diagnosed ice crystal number concentration formed by (c) homogeneous nucleation ( $\text{cm}^{-3}$ ) and (d) heterogeneous nucleation ( $\text{cm}^{-3}$ ).

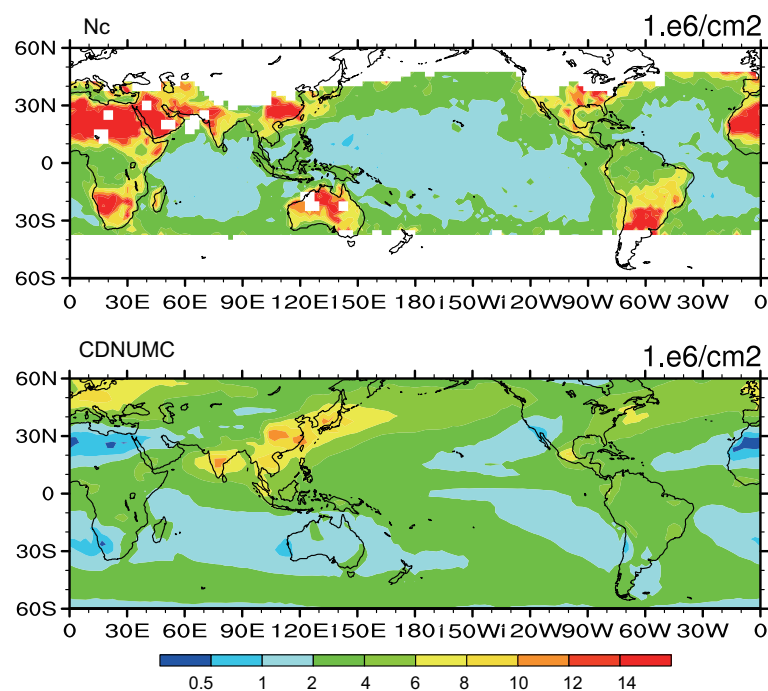


**Fig. 5.** Annual mean  $60^{\circ}\text{S}$  to  $60^{\circ}\text{N}$  column cloud droplet number concentrations (CDNUMC,  $1 \times 10^6 \text{ cm}^{-2}$ ) from AVHRR data (upper panel) and GAMIL-MG simulation (lower panel).

tration formed by homogeneous nucleation is significantly larger than heterogeneous nucleation in the upper troposphere. Thus, homogeneous nucleation is the dominant contributor to ice number concentration in the upper troposphere. Figure 4d shows that the ice number concentrations formed by heterogeneous nucleation are higher with high aerosol loading in the NH.

### 3.5 Column-integrated cloud droplet number concentration

Figure 5 shows CDNUMC from the GAMIL-MG simulation and the AVHRR retrievals (Han et al., 1998). The CDNUMC from GAMIL-MG simulation are higher in Europe, East Asia, and North America (lower panel). The higher CDNUMC in these regions reflects the higher aerosol loading. The CDNUMC from

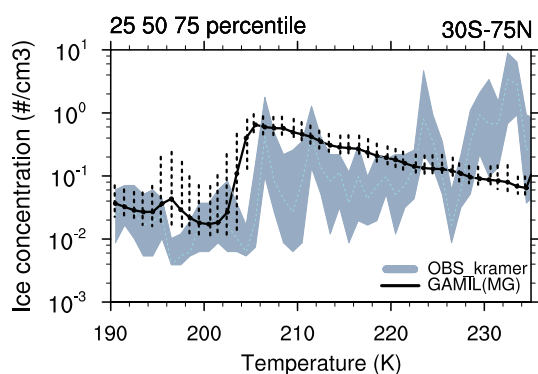


**Fig. 6.** In-cloud ice crystal number concentration ( $\text{cm}^{-3}$ ) versus temperature. Model results are sampled every three hours over tropical, mid-latitude and Arctic regions including the observation locations reported in Krämer et al. (2009). The 50% percentile (solid line), 25% and 75% percentiles (error bar) are shown for each 1-K temperature bin. The gray color indicates observations between 25% and 75% percentiles.

GAMIL-MG simulation is significantly lower in the SH than the NH. The CDNUMC is low over Sahara desert in the model, although the AVHRR data has anomalously high CDNUMC over deserts, which Han et al. (1998) attributed to incorrectly retrieving dust particles as cloud droplets. In addition to desert regions, CDNUMC retrieved from AVHRR data are also higher over East Asia and North America. Overall, the CDNUMC from model results has a pattern similar to that of AVHRR retrievals.

### 3.6 Ice crystal number concentration versus temperature

Figure 6 shows the cloud ice number concentration versus temperature from the GAMIL-MG model results and in situ measurements. Krämer et al. (2009) presented an extensive dataset of in situ aircraft observations of ice number concentrations. The most obvious feature of observations is that ice crystal number concentration is sharply decreased when the temperature fell below 205 K because homogeneous freezing was shut down artificially. Therefore, the simulated ice number concentration shows good agreement with observations. This result indicates that, in the global model, only heterogeneous nucleation scenarios would result in ice number concentration close to observations. Furthermore, the observed ice number concentration decreases with increasing temperature in the temperature range 205–220 K, with a median value  $\sim 0.5 \text{ cm}^{-3}$  at 205 K and  $\sim 0.05 \text{ cm}^{-3}$  at 220 K. The simulated ice number concentration also decreases with increasing temperature in this temperature range. This feature can be explained by that the

homogeneous freezing rate decrease with increasing temperature due to the lower frequency of reaching the ice supersaturation threshold (Fig. 4a). However, the GAMIL-MG simulation overestimates ice number concentration by approximately one order of magnitude at this temperature range. As shown in section 4.3, this bias can be removed by considering pre-existing ice crystals. Finally, the observed ice crystal number concentration increases with increasing temperature in the temperature range 220–235 K, the probable reason for which could be due to the shattering of ice crystals on the instrument inlets at these warmer temperatures (Jensen et al., 2010). Except for this temperature range, the simulated ice number concentrations are in reasonable agreement with observations.

## 4. Sensitivity test

Here we examine the sensitivity of simulated radiative fluxes and cloud fields to a variety of assumptions used in this new two-moment stratiform cloud microphysics scheme: different formulation for ice crystals formation in mixed-phase cloud, different droplet nucleation parameterization and ice nucleation parameterization. Each simulation is run for two years after a model spin-up of four months.

### 4.1 Different heterogeneous ice nucleation formulations in mixed-phase clouds

In mixed-phase clouds, ice formation is represented by heterogeneous ice nucleation of cloud droplets. Several heterogeneous nucleation formulations have been added to the GAMIL model to examine the uncertainties with heterogeneous ice nucleation parameterizations. In this study, we perform four sensitivity experiments using different heterogeneous nucleation formulations: Cooper, PDA, CNT, and Meyers.

Figure 7 shows the ice crystal number concentrations in mixed-phase clouds from sensitivity experiments. Both Cooper and Meyers formulations are a function of temperature or ice supersaturation, which are not related to aerosols. The ice number concentrations calculated from the Meyers formulation is similar to Cooper formulation in low temperature range ( $-40^{\circ}\text{C}$ – $-25^{\circ}\text{C}$ ). However, ice number concentrations calculated using the Meyers formulation are  $\sim 10$  times higher than those calculated using Cooper formulation between  $-20^{\circ}\text{C}$  and  $0^{\circ}\text{C}$ . Thus, the ice number concentrations in the middle and lower mixed-phase clouds from Meyers simulation are higher than those from Cooper simulation. Unlike Cooper and Meyers formulations, CNT, and PDA formulations link IN number to dust aerosol. As a result, ice number concentrations from both CNT and PDA simulations

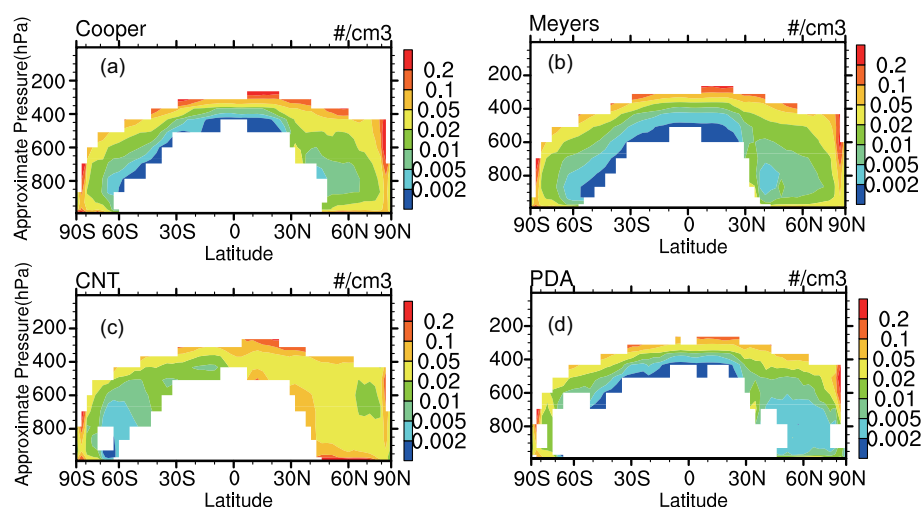


**Fig. 7.** Ice crystal number concentration in mixed-phased cloud ( $\text{cm}^{-3}$ ) calculated by different heterogeneous freezing formulations: (a) Cooper, (b) Meyers, (c) CNT, and (d) PDA.

are higher over NH. In addition, ice number concentrations calculated from Meyers or CNT formulation are  $\sim 10$  times larger than those from PDA. Thus, the ice number concentrations from PDA simulation are smaller than those of CNT and Meyer.

An overview of various global annual mean analyses is provided in Table 3. The global average PRECT and PRECL are similar in these four simulations. However, the LWP differences reach  $12 \text{ g m}^{-2}$  between these four simulations. PDA simulation has the largest LWP ( $74.7 \text{ g m}^{-2}$ ), and Meyers simulation has the smallest LWP ( $62.1 \text{ g m}^{-2}$ ). This phenomenon can be explained by that the precipitation formation via the ice phase is more efficient than in warm clouds, mixed-phase clouds with higher ice number concentration have a shorter lifetime than these clouds with lower ice number concentration (Lohmann and Hoose, 2009). Furthermore, PDA simulation has the strongest cloud forcing (both SWCF and LWCF), followed by the slightly weaker cloud forcing from the Cooper sim-

ulation and then much weaker cloud forcing from CNT and Meyers simulations. These results are consistent with the difference in LWP between these simulations. The SWCF difference ( $\leq 3.7 \text{ W m}^{-2}$ ) between these simulations highlights the importance of quantifying the heterogeneous IN number concentrations in mixed-phase clouds. Notably, the increase in ice crystal number concentrations in mixed-phase clouds can cause a decrease in SWCF. This result indicates that aerosol indirect effects on mixed-phase clouds can partly offset the aerosol indirect effects on warm clouds.

#### 4.2 Sensitivity to cloud droplet activation parameterizations

The two-moment MG cloud microphysics scheme in GAMIL includes two physically-based droplet nucleation parameterizations: AG and NS. Thus, the GAMIL model can be used to compare the aerosol indirect effects predicted using each parameterization while keeping other model parameters the same. Figure 8 illustrates the annual mean CDNUMC calculated using AG and NS parameterizations. The CDNUMC predicted by both AG and NS parameterizations are higher in the NH downwind of aerosol sources over Europe, East Asia, and North America. The CDNUMC calculated by the AG parameterization is slightly larger than that from NS in the regions mentioned here. This difference occurs because that the AG parameterization activates more aerosol particles than NS under high aerosol conditions (Ghan et al., 2011). However, the AG parameterization activates less aerosol particles than NS parameterization under low aerosol conditions (Ghan et al., 2011). Therefore, the CDNUMC calculated by the AG parameterization

**Table 3.** As Table 2 for sensitivity experiments in mixed-phase clouds using different heterogeneous freezing formulation.

Simulations	Cooper	Meyers	PDA	CNT
LWP	68.6	62.1	74.7	64.1
IWP	4.96	5.01	4.32	4.79
CDNUMC	2.77	2.63	2.94	2.57
SWCF	-52.4	-50.8	-54.5	-51.2
LWCF	23.9	23.1	24.9	23.4
CLDTOT	55.2	55.4	54.9	55.5
PRECL	0.58	0.56	0.58	0.57
PRECT	3.01	3.01	3.00	3.02

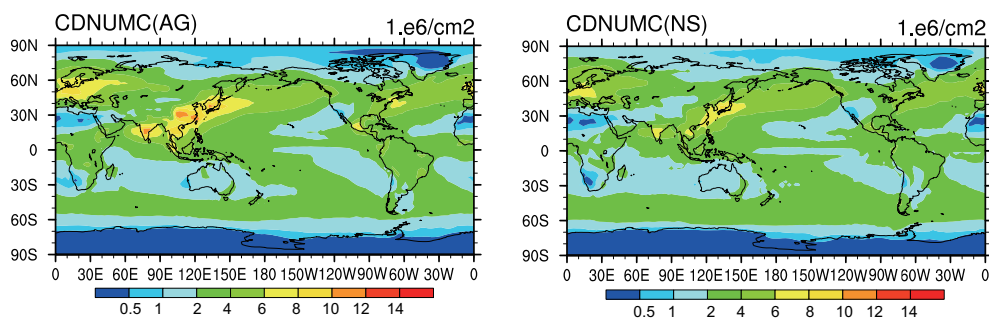


**Fig. 8.** Column cloud droplet number concentration ( $10^6 \text{ cm}^{-2}$ ) using AG parameterization (left) and NS parameterization (right).

is less than that using NS parameterization in the SH oceanic regions. In summary, the CDNUMC calculated using NS parameterization has the same pattern as AG parameterization. Furthermore, the global mean SWCF estimated from these two parameterizations are similar:  $-51.85 \text{ W m}^{-2}$  with AG and  $-51.82 \text{ W m}^{-2}$  with NS.

The anthropogenic aerosol indirect effect on warm clouds in GAMIL model has also been investigated. The annual global mean changes in SECF from preindustrial times to present day estimated from these two parameterizations are remarkably similar (Shi et al., 2010).

#### 4.3 Sensitivity of ice crystal number concentrations in cirrus clouds to ice nucleation parameterizations

The newly developed GAMIL model includes two physically-based ice nucleation parameterizations: LP and BN. We first compare the ice crystal number concentration calculated using the LP parameterization (simulation LP) with that calculated using the BN parameterization with the CNT formulation (simulation

BN) in the default model configuration. To estimate the effects of glassy aerosols, these two simulations do not take sulfate aerosols as glassy solids at low temperature ( $<205 \text{ K}$ ). Furthermore, ice nucleation parameterization (either LP or BN) are applied to both new and old clouds in the default configuration. However, in old clouds, if the pre-existing ice crystal number concentration is high enough, it would deplete the water vapor and hinder homogeneous freezing. In order to take into account the effects of pre-existing ice crystals on ice nucleation, in the sensitivity test of the Existing run, which is based on BN simulation, homogeneous freezing is not allowed to occur if the grid-box ice number concentration is  $>10^{-2} \text{ cm}^{-3}$  (Spichtinger and Gierens, 2009).

Ice crystal number concentration versus temperature from all sensitivity tests is shown in Fig. 9. Ice crystal number concentration in LP simulation is significantly less than that in BN simulation in the temperature range 200–230 K. The reason for this difference is that the occurrence frequency of homogeneous freezing in LP simulation is less than BN simulation, which can be partly explained by the large difference in computing IN number concentration (Fig. 10). At low temperatures ( $<205 \text{ K}$ ), ice crystal number concentrations in both LP and BN simulations are overestimated by approximately one order of magnitude. Compared with the reference simulation (GAMIL-MG simulation, Fig. 6), ice crystal number concentration would have compared well with in situ observations if homogeneous freezing is prevented from glassy solids. Compared with the BN simulation, ice crystal number concentration from the Existing simulation is in better agreement with observations in the temperature range 205–220 K. This suggests that impact of pre-existing ice crystals on homogeneous freezing in old clouds should be considered in global models. Because the lower ice crystal number concentration results in the larger ice crystal size and higher sedimentation rate, and thus a smaller IWP, IWP from Existing simulation is 30% smaller than that from BN

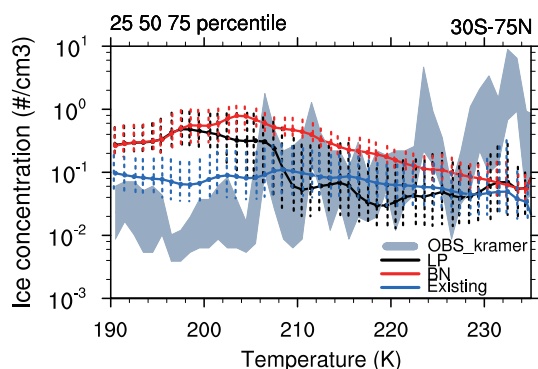


**Fig. 9.** The same as Fig. 6 but for sensitivity tests: using LP parameterization (LP: black), using BN parameterization (BN: red) and considering pre-existing ice crystals (Existing: blue).

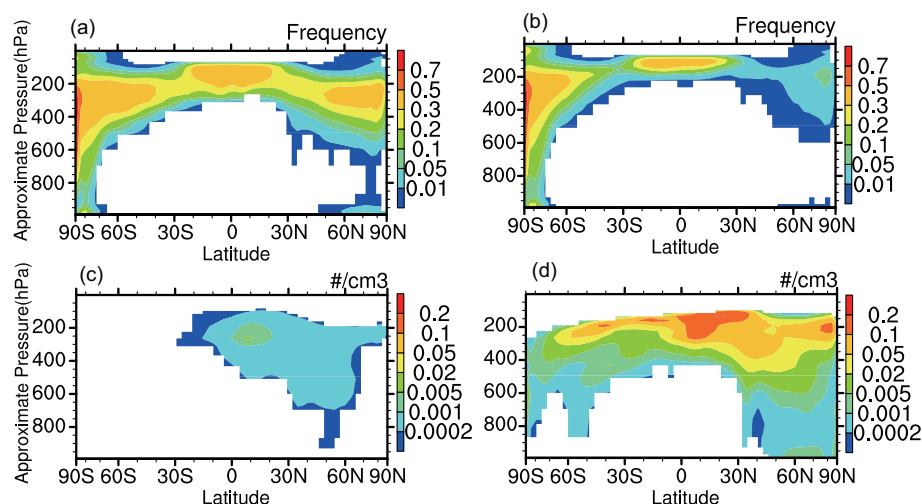


**Fig. 10.** Occurrence frequency of homogeneous nucleation using (a) BN parameterization and (b) LP parameterization. Diagnosed ice crystal number concentration formed by heterogeneous nucleation using (c) BN parameterization and (d) LP parameterization.

simulation. As a result of the lower IWP and the larger ice crystal size, cloud forcings (both LWCD and SWCF) from Existing simulation are weaker than those from the BN simulation.

## 5. Conclusions and discussions

To enhance the model's capability for studying aerosol indirect effects, a two-moment bulk stratiform cloud microphysics scheme and some recent developed droplet nucleation parameterizations and ice nucleation parameterizations have been implemented in GAMIL. Various aspects of the new GAMIL-MG model are evaluated with satellite and in situ observations. The global mean LWP in the GAMIL-MG model is increased to  $67.1 \text{ g m}^{-2}$ , within the range of uncertainty from SSM/I data ( $63\text{--}81 \text{ g m}^{-2}$ ). The global mean LWCF is  $22.5 \text{ W m}^{-2}$ , which is at the lower end of the range of estimates from various satellite observations ( $22\text{--}31 \text{ W m}^{-2}$ ). The global mean SWCF, which is underestimated in the standard GAMIL, is increased by 30%. The increased SWCF ( $-51.5 \text{ W m}^{-2}$ ) is in better agreement with observations ( $-46\text{--}53 \text{ W m}^{-2}$ ). The number concentration of liquid droplets and ice crystals, which is not linked to aerosols in the standard GAMIL, is then calculated from physically-based droplet nucleation parameterization and ice nucleation parameterization. The CDNUMC from the GAMIL-MG are higher in the NH downwind of aerosol sources over Europe, East Asia, and North America. The simulated CDNUMC has a pattern similar to that of the AVHRR retrievals. Additionally, simulated ice crystal number concentration

qualitatively agrees with in situ observations in the temperature range  $190\text{--}220 \text{ K}$ . Furthermore, the new GAMIL-MG represents a reasonable vertical structure of particle size and in-cloud number concentration.

There are several heterogeneous ice nucleation formulations in mixed-phase clouds. Sensitivity tests show that the global average PRECT and PRECT do not appear to be sensitive to different heterogeneous nucleation formulations. However, LWP is sensitive to different heterogeneous nucleation formulations. The simulation (Meyers) with high ice crystal number concentrations in mixed-phase clouds gives less LWP and weaker cloud forcing (both SWCF and LWCF). This suggests that aerosol indirect effects on mixed-phase clouds can partly offset the aerosol indirect effects on warm clouds.

The newly developed GAMIL-MG model includes two physically-based droplets nucleation parameterizations: AG and NS. Sensitivity tests show that the CDNUMC calculated using the NS parameterization has the same pattern as the AG parameterization. The global mean SWCF estimated from these two parameterizations are also similar:  $-51.85 \text{ W m}^{-2}$  with AG and  $-51.82 \text{ W m}^{-2}$  with NS. Therefore, we conclude that physically-based droplet nucleation parameterizations can provide a robust representation of aerosol activation process in climate models.

The new GAMIL-MG includes two physically-based ice nucleation parameterizations: LP and BN. Unlike droplet nucleation, there is a large difference in ice crystal number concentrations between LP and BN simulations, due to the large difference in diagnosed heterogeneous IN number concentrations. Compared

with the control simulation (GAMIL-MG), ice crystal number concentrations compare well with in situ observations when homogeneous freezing is prevented from glassy solids blow 205 K. Sensitivity tests also suggest that the impact of pre-existing ice crystals on homogeneous freezing in old clouds should be taken into account.

An important disadvantage of the present model setup is that the growth of ice particles in cirrus clouds is diagnosed by the fractional cloud closure scheme rather than water vapor deposition scheme. We plan to remove this disadvantage by adding a statistical cirrus cloud scheme in the future, following the approach of Wang and Penner (2010).

**Acknowledgements.** The authors thank Q. HAN for supplying AVHRR data. This work was supported by the National Natural Science Funds of China (Grant No.41205071) and the Ministry of Science and Technology of China for the National Basic Research Program of China (973 Program: Grant No. 2011CB309704). X. Liu also would like to acknowledge the funding support from the U.S. Department of Energy (DOE), Office of Science, Earth System Modeling Program.

## REFERENCES

- Abdul-Razzak, H., and S. J. Ghan, 2000: A parameterization of aerosol activation 2. Multiple aerosol types. *J. Geophys. Res.*, **105**(D5), 6837–6844.
- Adler, R. F., and Coauthors, 2003: The version-2 global precipitation climatology project (GPCP) monthly precipitation analysis (1979–Present). *Journal of Hydrometeorology*, **4**, 1147–1167.
- Arakawa, A., 2004: The cumulus parameterization problem: Past, present, and future. *J. Climate*, **17**(3), 2493–2525.
- Barahona, D., and A. Nenes, 2008: Parameterization of cirrus cloud formation in large-scale models: Homogeneous nucleation. *J. Geophys. Res.*, **113**(D11), doi: 10.1029/2007jd009355.
- Barahona, D., and A. Nenes, 2009a: Parameterizing the competition between homogeneous and heterogeneous freezing in cirrus cloud formation—monodisperse ice nuclei. *Atmos. Chem. Phys.*, **9**(2), 369–381.
- Barahona, D., and A. Nenes, 2009b: Parameterizing the competition between homogeneous and heterogeneous freezing in ice cloud formation—polydisperse ice nuclei. *Atmos. Chem. Phys.*, **9**(16), 5933–5948.
- Collins, W. D., P. J. Rasch, B. E. Eaton, B. Khattatov, J. F. Lamarque, and C. S. Zender, 2001: Simulating aerosols using a chemical transport model with assimilation of satellite aerosol retrievals: Methodology for INDOEX. *J. Geophys. Res.*, **106**, 7313–7336.
- Collins, W. D., and Coauthors, 2006: The community climate system model version 3 (CCSM3). *J. Climate*, **19**(11), 2122–2143.
- Cooper, W. A., 1986: Ice initiation in natural clouds. precipitation enhancement—a scientific challenge. *Meteorological Monographs*, **21**, 29–32.
- Demott, P. J., M. P. Meyers, and W. R. Cotton, 1994: Parameterization and impact of ice initiation processes relevant to numerical-model simulations of cirrus clouds. *J. Atmos. Sci.*, **51**(11), 1577–1577.
- Demott, P. J., D. C. Rogers, and S. M. Kreidenweis, 1997: The susceptibility of ice formation in upper tropospheric clouds to insoluble aerosol components. *J. Geophys. Res.*, **102**(D16), 19575–19584.
- Froyd, K. D., D. M. Murphy, T. J. Sanford, D. S. Thomson, J. C. Wilson, L. Pfister, and L. Lait, 2009: Aerosol composition of the tropical upper troposphere. *Atmos. Chem. Phys.*, **9**, 4363–4385.
- Gensch, I. V., and Coauthors, 2008: Supersaturations, microphysics and nitric acid partitioning in a cold cirrus cloud observed during CR-AVE 2006: An observation-modelling intercomparison study. *Environmental Research Letters*, **3**, doi: 10.1088/1748-9326/3/3/035003.
- Gettelman, A., H. Morrison, and S. J. Ghan, 2008: A new two-moment bulk stratiform cloud microphysics scheme in the community atmosphere model, version 3 (CAM3). Part II: Single-column and global results. *J. Climate*, **21**(15), 3660–3679, doi: 10.1175/2008jcli2116.1.
- Gettelman, A., and Coauthors, 2010: Global simulations of ice nucleation and ice supersaturation with an improved cloud scheme in the community atmosphere model. *J. Geophys. Res.*, **115**(D18), D18216, doi: 10.1029/2009jd013797.
- Ghan, S. J., and S. E. Schwartz, 2007: Aerosol properties and processes—A path from field and laboratory measurements to global climate models. *Bull. Amer. Meteor. Soc.*, **88**(7), 1059–1083, doi: 10.1175/Bams-88-7-1059.
- Ghan, S. J., and Coauthors, 2011: Droplet nucleation: Physically-based parameterizations and comparative Evaluation. *Journal of Advances in Modeling Earth Systems*, **3**(M10001), doi: 10.1029/2011ms000074.
- Greenwald, T. J., G. L. Stephens, T. H. V. Haar, and D. L. Jackson, 1993: A physical retrieval of cloud liquid water over the global oceans using special sensor microwave/imager (SSM/I) observations. *J. Geophys. Res.*, **98**, 18471–18488.
- Hahn, C. J., S. G. Warren, and J. London, 1994: Climatological data for clouds over the globe from surface observations, 1982–1991: The total cloud edition. Tech. Rep., NDP026A, 42pp.
- Han, Q., W. B. Rossow, J. Chou, and R. W. Welch, 1998: Global variation of column droplet concentration in low-level clouds. *Geophys. Res. Lett.*, **25**, 1419–1422.
- Iacono, M. J., J. S. Delamere, E. J. Mlawer, M. W. Shephard, S. A. Clough, and W. D. Collins, 2008: Radiative forcing by long-lived greenhouse gases: Calculations with the AER radiative transfer models. *J. Geophys. Res.*, **113**(D13103), doi: 10.1029/2007jd009355.

- 10.1029/2008JD009944.
- IPCC, 2007: *Climate Change 2007: The Physical Basis. Contribution of Working Group I to the Fourth Assessment Report of the Intergovernmental Panel on Climate Change*, S. Solomon et al., Eds., Cambridge University Press, New York, 996pp.
- Jensen, E. J., L. Pfister, T. P. Bui, P. Lawson, and D. Baumgardner, 2010: Ice nucleation and cloud microphysical properties in tropical tropopause layer cirrus. *Atmos. Chem. Phys.*, **10**(3), 1369–1384.
- King, M. D., and Coauthors, 2003: Cloud and aerosol properties, precipitable water, and profiles of temperature and water vapor from MODIS. *IEEE Trans. Geosci. Remote Sens.*, **41**, 442–458.
- Kohler, H., 1921: Zur kondensation des wasserdampfe in der atmosphäre. *Geophys. Publ.*, **2**, 3–15.
- Krämer, M., and Coauthors, 2009: Ice supersaturations and cirrus cloud crystal numbers. *Atmos. Chem. Phys.*, **9**(11), 3505–3522.
- Li, L., B. Wang, Y. Wang, and H. Wan, 2007: Improvements in climate simulation with modifications to the Tiedtke convective parameterization in the grid-point atmospheric model of IAP LASG (GAMIL). *Adv. Atmos. Sci.*, **24**(2), 323–335, doi: 10.1007/s00376-007-0323-3.
- Li, L., Y. Wang, B. Wang, and T. Zhou, 2008: Sensitivity of the grid-point atmospheric model of IAP LASG (GAMIL1.1.0) climate simulations to cloud droplet effective radius and liquid water path. *Adv. Atmos. Sci.*, **25**(4), 529–540, doi: 10.1007/s00376-008-0529-z.
- Li, L., and Coauthors, 2013: Evaluation of grid-point atmospheric model of IAP LASG version 2 (GAMIL2). *Adv. Atmos. Sci.*, doi: 10.1007/s00376-013-2157-5.
- Lin, S.-J., and R. B. Rood, 1996: Multidimensional flux-form semi-Lagrangian transport schemes. *Mon. Wea. Rev.*, **124**, 2046–2070.
- Liu, X., J. E. Penner, S. J. Ghan, and M. Wang, 2007: Inclusion of ice microphysics in the NCAR community atmospheric model version 3 (CAM3). *J. Climate*, **20**(18), 4526–4547, doi: 10.1175/Jcli4264.1.
- Liu, X. H., and J. E. Penner, 2005: Ice nucleation parameterization for global models. *Meteor. Z.*, **14**(4), 499–514, doi: 10.1127/0941-2948/2005/0059.
- Loeb, N. G., B. A. Wielicki, D. R. Doelling, G. L. Smith, D. F. Keyes, S. Kato, N. Manalo-Smith, and T. Wong, 2009: Toward optimal closure of the Earth's top-of-atmosphere radiation budget. *J. Climate*, **22**, 748–766.
- Lohmann, U., 2008: Global anthropogenic aerosol effects on convective clouds in ECHAM5-HAM. *Atmos. Chem. Phys.*, **8**(7), 2115–2131, doi: 10.5194/acp-8-2115-2008.
- Lohmann, U., and J. Feichter, 2005: Global indirect aerosol effects: A review. *Atmos. Chem. Phys.*, **5**, 715–737.
- Lohmann, U., and C. Hoose, 2009: Sensitivity studies of different aerosol indirect effects in mixed-phase clouds. *Atmos. Chem. Phys.*, **9**(22), 8917–8934.
- Lohmann, U., P. Stier, C. Hoose, S. Ferrachat, S. Kloster, E. Roeckner, and J. Zhang 2007: Cloud microphysics and aerosol indirect effects in the global climate model ECHAM5-HAM. *Atmos. Chem. Phys.*, **7**(13), 3425–3446.
- Meyers, M. P., P. J. Demott, and W. R. Cotton, 1992: New primary ice-nucleation parameterizations in an explicit cloud model. *J. Appl. Meteor.*, **31**(7), 708–721.
- Meyers, M. P., R. L. Walko, J. Y. Harrington, and W. R. Cotton, 1997: New RAMS cloud microphysics parameterization.2. The two-moment scheme. *Atmospheric Research*, **45**(1), 3–39.
- Morrison, H., and J. O. Pinto, 2005: Mesoscale modeling of springtime Arctic mixed-phase stratiform clouds using a new two-moment bulk microphysics scheme. *J. Atmos. Sci.*, **62**, 3683–3704.
- Morrison, H., and A. Gettelman, 2008: A new two-moment bulk stratiform cloud microphysics scheme in the community atmosphere model, version 3 (CAM3). Part I: Description and numerical tests. *J. Climate*, **21**(15), 3642–3659, doi: 10.1175/2008jcli2105.1.
- Nenes, A., and J. H. Seinfeld, 2003: Parameterization of cloud droplet formation in global climate models. *J. Geophys. Res.*, **108**, doi: 10.1029/2002JD002911.
- Phillips, V. T. J., L. J. Donner, and S. T. Garner, 2007: Nucleation processes in deep convection simulated by a cloud-system-resolving model with double-moment bulk microphysics. *J. Atmos. Sci.*, **64**(3), 738–761, doi: 10.1175/Jas3869.1.
- Phillips, V. T. J., P. J. DeMott, and C. Andronache, 2008: An empirical parameterization of heterogeneous ice nucleation for multiple chemical species of aerosol. *J. Atmos. Sci.*, **65**(9), 2757–2783, doi: 10.1175/2007jas2546.1.
- Pruppacher, H. R., and J. D. Klett, 1997: *Microphysics of Cloud and Precipitation*. Springer, New York, 954pp.
- Rasch, P. J., and J. E. Kristjánsson, 1998: A comparison of the CCM3 model climate using diagnosed and predicted condensate parameterizations. *J. Climate*, **11**, 1587–1614.
- Rossow, W. B., and R. A. Schiffer, 1999: Advances in understanding clouds from ISCCP. *Bull. Amer. Meteor. Soc.*, **80**, 2261–2287.
- Salzmann, M., Y. Ming, J.-C. Golaz, P. A. Ginoux, H. Morrison, A. Gettelman, M. Krämer, and L. J. Donner, 2010: Two-moment bulk stratiform cloud microphysics in the GFDL AM3 GCM: Description, evaluation, and sensitivity tests. *Atmos. Chem. Phys. Discuss*, **10**, 6375–6446..
- Scott, N. A., and Coauthors, 1999: Characteristics of the TOVS pathfinder Path-B dataset. *Bull. Amer. Meteor. Soc.*, **80**, 2679–2701.
- Shi, X.-J., B. Wang, X.-H. Liu, M.-H. Wang, L.-J. Li, and L. Dong, 2010: Aerosol indirect effects on warm clouds in the grid-point atmospheric model of IAP LASG (GAMIL). *Atmos. Oceanic Sci. Lett.*, **3**(4), 237–241.

- Slingo, J. M., 1987: The development and verification of a cloud prediction scheme for the ECMWF model. *Quart. J. Roy. Meteor. Soc.*, **113**(477), 899–927.
- Spichtinger, P., and K. M. Gierens, 2009: Modelling of cirrus clouds—Part 2: Competition of different nucleation mechanisms. *Atmos. Chem. Phys.*, **9**, 2319–2334.
- Storelvmo, T., J. E. Kristjansson, and U. Lohmann, 2008: Aerosol influence on mixed-phase clouds in CAM-Oslo. *J. Atmos. Sci.*, **65**, 3214–3230.
- Storelvmo, T., U. Lohmann, and R. Bennartz, 2009: What governs the spread in shortwave forcings in the transient IPCC AR4 models? *Geophys. Res. Lett.*, **36**, doi: 10.1029/2008gl036069.
- Tiedtke, M., 1989: A comprehensive mass flux scheme for cumulus parameterization in large-scale models. *Mon. Wea. Rev.*, **117**, 779–800.
- Vavrus, S., and D. Waliser, 2008: An improved parameterization for simulating Arctic cloud amount in the CCSM3 climate model. *J. Climate*, **21**, 5673–5687.
- Wang, M., and J. E. Penner, 2010: Cirrus clouds in a global climate model with a statistical cirrus cloud scheme. *Atmos. Chem. Phys.*, **10**(2), 5449–5474.
- Weng, F. Z., and N. C. Grody, 1994: Retrieval of cloud liquid water using the special sensor microwave imager (SSM/I). *J. Geophys. Res.*, **99**, 25535–25551.
- Wu, Z., and J. Li, 2008: Prediction of the Asian-Australian monsoon interannual variations with the grid-point atmospheric model of IAP LASG (GAMIL). *Adv. Atmos. Sci.*, **25**(3), 387–394.
- Xie, P. P., P. A. Arkin, 1997: Global precipitation: a 17-year monthly analysis based on gauge observations, satellite estimates, and numerical model outputs. *Bull. Amer. Meteor. Soc.*, **78**, 2539–2558.
- Yang, J., B. Wang, Y. Guo, H. Wan, and Z. Ji, 2007: Comparison between GAMIL, and CAM2 on interannual variability simulation. *Adv. Atmos. Sci.*, **24**(1), 82–88.
- Zhang, G. J., and N. A. McFarlane, 1995: Sensitivity of climate simulations to the parameterization of cumulus convection in the Canadian climate centre general circulation model. *Atmos.–Ocean*, **33**, 407–446.
- Zhang, G. J., and M. Mu, 2005: Effects of modifications to the Zhang-McFarlane convection parameterization on the simulation of the tropical precipitation in the national center for atmospheric research community climate model, version 3. *J. Geophys. Res.*, **110**(D9), D09109, doi: 10.1029/2004jd005617.
- Zhang, K., 2008: Tracer transport evaluation and aerosol simulation with the atmospheric model GAMIL-LIAM., Ph.D. thesis, Institute of Atmospheric Physics, Chinese Academy of Sciences, 139pp.